Published in final edited form as:
Bioconjug Chem. 2008 April ; 19(4): 866–875. doi:10.1021/bc700390r.

Unnatural Amino Acid Incorporation into Virus-Like Particles

Erica Strable[†], **Duane E. Prasuhn Jr.**[†], **Andrew K. Udit**[†], **Steven Brown**[†], **A. James Link**[‡], **John T. Ngo**[‡], **Gabriel Lander**[§], **Joel Quispe**[§], **Clinton S. Potter**[§], **Bridget Carragher**[§], **David A. Tirrell**[‡], and **M. G. Finn**[*,†]
Department of Chemistry and The Skaggs Institute of Chemical Biology, and National Resource for Automated Molecular Microscopy and Department of Cell Biology, The Scripps Research Institute, La Jolla, California 92037, and Division of Chemistry and Chemical Engineering, California Institute of Technology, Pasadena, California 91125. Received October 21, 2007; Revised Manuscript Received January 14, 2008

Abstract

Virus-like particles composed of hepatitis B virus (HBV) or bacteriophage Q*β* capsid proteins have been labeled with azide- or alkyne-containing unnatural amino acids by expression in a methionine auxotrophic strain of *E. coli*. The substitution does not affect the ability of the particles to self-assemble into icosahedral structures indistinguishable from native forms. The azide and alkyne groups were addressed by Cu(I)-catalyzed [3 + 2] cycloaddition: HBV particles were decomposed by the formation of more than 120 triazole linkages per capsid in a location-dependent manner, whereas Q*β* suffered no such instability. The marriage of these well-known techniques of sense-codon reassignment and bioorthogonal chemical coupling provides the capability to construct polyvalent particles displaying a wide variety of functional groups with near-perfect control of spacing.

INTRODUCTION

A variety of strategies and expression systems have been employed to cotranslationally incorporate unnatural amino acids into proteins. The three most common approaches are the use of a nonsense or rare codon (1-8), the use of a larger (quadruplet) codon (4,9), or the reassignment of a sense codon (10-17). In the last approach, codons for methionine (11-15, 18,19), leucine (20), isoleucine (21), phenylalanine (22), tryptophan (23,24), and proline (25) have been used for incorporation of unnatural amino acids. Here we employ this technique (10,16,26) to replace methionine with the unnatural amino acids azidohomoalanine (**1**, Figure 1) and homopropargyl glycine (**2**) for the first time in proteins that spontaneously assemble into virus-like particles in the host *E. coli* cell.

The incorporation of organic azides and terminal alkynes introduces highly energetic functional groups that are inert to biological molecules under physiological conditions. The azide group's "bio-orthogonality" has been particularly prized, due to its participation in the Staudinger reaction with phosphines (27,28), cycloaddition with strained-ring alkynes (27,29-31), and

* E-mail: mgfinn@scripps.edu..
[†]Department of Chemistry and The Skaggs Institute of Chemical Biology,The Scripps Research Institute.
[‡]California Institute of Technology.
[§]National Resource for Automated Molecular Microscopy and Department of Cell Biology, The Scripps Research Institute.

Supporting Information Available: Details of protein expression, characterization of alkyne-labeled particles, and summary of previously reported yields of proteins incorporating unnatural amino acids. This material is available free of charge via the Internet at http://pubs.acs.org.

copper(I)-mediated cycloaddition with terminal alkynes (32,33). We have developed the last of these into a robust tool for making connections with biological molecules (34) at reasonable concentrations (35). The process has been used by us and others for the selective modification of enzymes (6,36), cells (14,15,37), virus particles (7,34,35,38,39), newly synthesized proteins (40-43), and tissue lysates (44,45). The cotranslational incorporation of azides and alkynes into self-assembled virus-like particles enables their use in the chemoselective preparation of polyvalently labeled structures. In addition to providing near-perfect control over the positioning of desired groups on the virus surface, the genetic incorporation and subsequent chemical addressing of azides and alkynes allows the independent use of other bioconjugation techniques without protecting group manipulations or concerns about cross-reactivity.

The inner protein shell (core antigen) of hepatitis B virus is composed of either 180 (maximum diameter 318 Å) or 240 (maximum diameter 348 Å) copies of the coat protein (Figure 2) (46, 47). We will use the abbreviation HBV to refer to the latter structure, which is the predominant (46) particle used here; the designation HBcAg also appears in the literature. The native capsid protein is 183 amino acids in length; we employed the assembly domain composed of the first 149 amino acids (Cp149), which is largely α-helical and produces more than 95% of the 240-subunit particle. While a variety of recombinant protein expression systems have been used successfully to produce the HBV core antigen (48,49), by far the most common has been *E. coli* (50,51).

The *E. coli* bacteriophage Q*β* is composed of 180 copies of the coat protein assembled into a $T = 3$ icosahedral virion (average diameter 270 Å, Figure 2) (52,53), encapsidating a positive-sense RNA genome (54). The capsid protein is composed of 132 amino acids of mostly antiparallel *β*-sheet structure (52,55). For a nonthermophile, the capsid is unusually stable toward extremes of pH, temperature, and chemical reagents, due to a combination of a large noncovalent contact area within capsid dimers. Furthermore, cysteine residues at positions 74 and 80, located at the five- and threefold axes of symmetry, respectively, form disulfide linkages to the corresponding residues of neighboring subunits. As a result, rings of five subunits are formed at the icosahedral fivefold symmetry axis, and rings of six protein subunits are formed around the threefold axis, with each protein dimer being linked to the capsid by four disulfide bonds. The coat protein of Q*β* is tolerant of genetic manipulation and can be recombinantly expressed in high yields (56-58), making it desirable for a variety of applications. All mention below of particles or virions refer to the noninfectious, self-assembled virus-like particles (VLPs) of either HBV or Q*β*, encapsidating random cellular RNA.

RESULTS AND DISCUSSION

Unnatural Amino Acid Incorporation

We have incorporated the unnatural amino acids azidohomoalanine (**1**) and homopropargylglycine (**2**) into HBV and Q*β* using reassignment of the methionine sense codon, which provides global replacement of all methionines with the unnatural amino acid. Thus, genetic engineering is usually required to place Met residues where the unnatural amino acids are desired. The presence of *N*-terminal methionine, required by the translational machinery, is variable for both HBV Cp149 and Q*β*, as it is for many proteins expressed in *E. coli* (60). HBV contains one additional Met at position 66, situated halfway up the side of the four helix bundle and therefore accessible to solution-phase reactants (Figure 2A). The Q*β* sequence has no other methionines, so mutants K16 M and T93 M were generated. The former places the new amino acid at the most exposed location of the capsid exterior, while the latter installs Met (or its surrogate) on the interior surface in a somewhat hindered position (Figure 2C).

For the efficient incorporation of unnatural amino acids, the protein must be expressed under tight inducible control. Native and mutant HBV and Q*β* coat protein sequences were cloned into the pQE-60 plasmid (Qiagen) and the methionine auxotroph *E. coli* strain M15(pREP4) MA was used for expression. The transformed cells were grown in minimal media supplemented with all 20 naturally occurring amino acids. When the desired mass of cells was achieved, methionine was removed from the media by pelleting, washing, and resuspending the cells in minimal media containing all the natural amino acids except methionine. The cells were incubated at 37 °C for 30−60 min to allow the bacteria to deplete their intracellular stocks of methionine. Finally protein expression was initiated by distributing the cells in minimal media containing the 19 natural amino acids, 1 mM isopropyl-*β*-D-1-thiogalactopyranoside (IPTG), and 80 mg/L of racemic **1** or **2**.

A series of control experiments established that HBV or Q*β* protein was produced only when the minimal media was supplemented by Met, **1**, or **2**, and only in the presence of IPTG. In media supplemented with **1** or **2**, the yield of isolated HBV or Q*β* particles was approximately 20−60% of the amount of protein produced in normal media under the same induction by IPTG (Table 1), representing some of the highest yields of unnatural amino acid-containing proteins reported thus far (see Supporting Information).

HBV and Q*β* VLPs containing **1** or **2** were indistinguishable in all physical characteristics from the analogous particles incorporating methionine (Figure 3). In each case, ultracentrifugation through sucrose gradients (not shown) and analysis on size-exclusion chromatography produced sharp virus bands at the same position as native capsids. Negative-stained transmission electron microscopy images of the particles revealed homogeneous samples of icosahedral nonaggregated particles. (The HBV Cp149 particles containing **1** do not contain nucleic acid, and thus exhibit stain uptake with dark centers. Q*β* particles are packed full of random cellular nucleic acid and have light centers in the negative stained images.) SDS-PAGE analyses revealed the same high purities of the capsids containing unnatural amino acids as those obtained with methionine. Last, the structures of both the HBV and Q*β* virus-like particles with **1** were confirmed by cryo-electron microscopy image reconstruction. The electron density maps overlaid well with the published X-ray crystal structures for the native capsids.

The incorporation of **1** and **2** in place of methionine was confirmed by trypsin digestion and analysis of the resulting peptides using MALDI mass spectrometry, with the results summarized in Figure 4. Sequence coverage of the wild-type and **1**-labeled HBV Cp149 particle was nearly complete, with all but two residues included (Ile97, Arg98). Following normal expression in the presence of all 20 amino acids, Met was found at positions 1 and 66, the former in 70−90% of the protein, varying from batch to batch. The same result was observed when **1** was substituted for Met in the protocol described above, with **1** incorporated at the *N*-terminus in 70−90% of the protein produced, and completely (>95%) at position 66. The mutation M66S was also constructed, and found to contain the same 70−90% of **1** at the *N*-terminus when expressed with the unnatural amino acid.

Analysis of Q*β* capsids required shorter trypsin digestion times to ensure limited proteolysis of the amino-terminal region. A coverage map that included all peptide fragments larger than three amino acids was obtained (Figure 4). Post-translational processing at the *N*-terminus was found to vary with the nature of the residue installed at that position. Under normal (Met-containing) expression, Met1 was never detected in either wild-type or mutant particles, showing that it was processed away during protein production (therefore, the amino acid numbering eliminates this residue). When **1** was substituted for Met in any form of the Q*β* sequence, approximately 10% of the capsids were found to have the unnatural amino acid at the *N*-terminus. However, in approximately one of every five batches this level of incorporation spiked to as much as 90%. It was therefore necessary to analyze each preparation of Q*β* capsids

to determine the number of azide-containing residues available for conjugation. Incorporation of **1** at either of the internal positions tested (16 or 93) was uniformly excellent (>95%). The same type of analysis (not shown) revealed 50% incorporation of **2** into Qβ K16 M at position 16, with the remainder being Met. No homopropargyl glycine was detected at position 1.

Conjugation to Genetically Incorporated Azide and Alkyne Groups

Since the expression of HBV in the presence of **1** provided 70−90% incorporation at position 1 and complete incorporation at position 66, a maximum of approximately 410−460 azides per VLP should be available for conjugation. We employed these particles as reagents in the copper-catalyzed azide-alkyne cycloaddition (CuAAC) reaction, using CuOTf and accelerating ligand **4** under inert atmosphere as has been previously described (61,62). The purified virus was pelleted out of solution, taken into an inert-atmosphere glovebox, and resuspended in degassed 0.1 M Tris buffer (pH 8.0) to prepare for reaction with fluorescein alkyne **3** under our standard conditions, as shown in Figure 5. After 16 h at room temperature, intact capsids could neither be detected by size-exclusion chromatography (Figure 6) nor recovered from sucrose gradients. However, gel electrophoresis (Figure 6) showed strong fluorescein labeling of the protein. Trypsin digestion and MALDI analysis in the manner described above revealed that approximately 50% of the sites at position 66 were labeled with fluorescein (equal intensities for the 56−81 fragment, m/z = 2919.3, and its labeled analogue with an increase in mass of 413 Da). Interestingly, fewer than 10% of the azide groups at position 1 were addressed.

HBV particles lacking incorporated azide groups were found to be stable toward the reaction conditions without coupling to fluorescein, ruling out nonspecific adsorption of the dye (Table 2, entry 1). All HBV particles were stable to the CuAAC reaction conditions (copper, ligand, buffer, and sample handling) and also toward extended incubation with fluorescein alkyne **3** in the absence of CuAAC catalyst. However, the particles did decompose when either ligand **4** or the previously used tris(triazolylmethyl)amine **5** was employed in the CuAAC process, showing that the nature of the ligand made no difference to particle stability. When the reaction time was varied, or the amount of catalyst was reduced, virus-like particles were recovered in yields inversely proportional to the amount of CuAAC reaction that had occurred. The use of rhodamine, biotin, or Gd(DOTA) reagents (**6**, **7**, or **8**) in place of fluorescein alkyne gave similar results. We therefore conclude that the decomposition of the particle was caused by the covalent attachment of these structures. We have previously observed other particles such as cowpea mosaic virus (CPMV) to be similarly sensitive to the covalent tethering of flat, hydrophobic species such ferrocene, tetramethylrhodamine, Fe(III) protoporphyrin IX, Ru(II) bipyridine complexes, and doxorubicin. However, the nature of the attached species varied somewhat in this case, and so it may well be that the triazole linkage, which is common to each of these examples, is responsible for the instability of the virus-like HBV particle. CPMV and Qβ have both been shown to be stable toward high levels of coverage by triazoles (34,35,37,38,62).

We attempted to strike a balance between covalent attachment and stability for HBV by varying the concentrations of CuOTf, ligand **4**, fluorescein-alkyne **3**, and protein. The use of 250 μM CuOTf with 500 μM ligand **4** slowed the reaction enough to allow the recovery of a maximum of 40% of the starting amount of capsids as intact icosahedra, bearing an average of 120 fluorescein molecules per capsid (Table 2, entry 2). The vast majority of these were attached to the M66 position and not to the *N*-terminal azidohomoalanine residue, as shown by trypsin digestion/MS. The loading value was determined by UV–vis absorbance spectroscopy of fluorescein (495 nm) in samples of purified labeled particles, with calibration using known samples under similar conditions (fluorescein in the presence of protein; protein concentrations determined by Lowry protein assay). It should also be noted that the attachment reaction was inhibited by the use of ligand **4** in greater than a 2:1 molar ratio with respect to Cu, consistent

with previous observations (61), and that higher concentrations of Cu catalyst **4** gave rise to greater amounts of capsid decomposition as the number of reactions climbed above the 120-per-particle level.

The site of bioconjugation was moved from the spike to the "floor" of the HBV structure by mutation of M66 to serine. Expression of the M66S Cp149 mutant in the presence of azidohomoalanine **1** allowed the isolation of a particle having reactive azide only at the *N*-terminus (70−90% incorporation, Table 1). Reaction with fluorescein-alkyne **3** under the conditions shown in Figure 5 gave rise to the same approximate loading of 120 per particle, but isolated in significantly higher yield (60−70%, which represents the maximum possible recovery at this scale due to losses in sample handling from sucrose gradient purification; Table 2, entry 3). Since the HBV particle bearing azidohomoalanine at both positions 1 and 66 showed predominant labeling at the latter, we conclude that the more exposed position on the 4-helix bundle is both more reactive and more deleterious to capsid stability when labeled. Decomposition of the particle results in denaturation and precipitation, and thus removal of protein from the labeling reaction. The greater capsid stability in the M66S case may derive from the fact that the *N*-terminus, now the only site bearing azide groups, is relatively far from the interface between subunit dimers. Compounds attached by flexible linkers to M66, in contrast, are positioned to easily interact with the hydrophobic interior of each 4-helix bundle. The potential for small molecules to affect HBV capsid assembly and stability by binding at subunit interfaces has been previously illustrated for certain dihydropyrimidine derivatives (63,64).

Qβ proved to be much more amenable to CuAAC derivatization. Each of the few azide groups in the wild-type virus-like particle containing **1** at 5−10% of the *N*-terminal sites was addressed with alkyne reagent **4** (Table 2, entry 5). When **1** was additionally installed at each of the highly exposed K16 M positions, the particle was also completely labeled with fluorescein, causing no apparent decomposition (Table 2, entry 6). A rare sample in which azidohomoalanine was largely retained at the *N*-terminus, designated Qβ $(1M\text{-}N_3)_{160}(K16M\text{-}N_3)_{180}$, took on 306 ± 30 dyes under standard conditions, and 330 ± 20 dyes in the presence of higher concentrations of protein and catalyst, all with excellent particle yield and stability (Table 2, entry 7). Loading values were determined with calibrated measurements of fluorescein absorbance and protein concentration determined by a modified Lowry assay, since the Qβ VLP contains no tryptophan residues, making for poor UV–vis absorbance characteristics. The resulting particles and protein were characterized in the same manner as HBV above (see Figure 3 for size-exclusion chromatography and gel electrophoresis). Trypsin digestion and mass spectrometry confirmed the loading values by showing the expected peptide fragments (and only those fragments) to be increased by 413 Da.

The accessibility of the $K16M\text{-}N_3$ insertion was further demonstrated by the chemoselective conjugation of a protein to the Q$\beta$$(1M\text{-}N_3)_{9–18}(K16M\text{-}N_3)_{180}$ particle. Transferrin, an 80 kD iron transport protein, was derivatized with *N*-propargylbromoacetamide and purified to give **9** (Figure 5), in analogous fashion to a maleimide-alkyne derivative previously described (35). The CuAAC reaction of **9** with Qβ $(1M\text{-}N_3)_{9–18}(K16M\text{-}N_3)_{180}$ gave a particle bearing covalently attached transferrin, as shown by gel electrophoresis and TEM (Figure 6).

Qβ $(1M\text{-}N_3)_{9–18}(T93M\text{-}N_3)_{180}$, in which the nonterminal unnatural amino acid is on the interior surface of the capsid, was not nearly as reactive as the K16 M derivative (Table 2, entry 8). While all of the *N*-terminal residues were coupled to **3** under standard CuAAC conditions, only 30−40 dyes were attached to the particle in total, which means that only 20−30 of the 180 azide-labeled T93 M sites participated in the reaction. As before, yields of intact particles were good. The same result was observed when alkyne **8** was used. Position 93 has both a more

congested protein environment than position 16, and may well be occluded by associated RNA packaged inside the particle, giving rise to sluggish reactivity.

Lastly, the alkyne-containing particle Qβ (K16M-CCH)$_{90}$ proved to be sensitive to the attachment of fluorescein azide **10** (Table 2, entry 9), giving rise to low recoveries of partially conjugated material. Note that azide **10**, and not alkyne **3**, induces instability in the resulting Qβ conjugate (each attached to unnatural amino acids installed at the same site). This is presumably a function of the longer tether between the reactive group and the fluorescein moiety in **10**, allowing the polycyclic aromatic structure to more easily interact with hydrophobic subunit interfaces in the particle. The use of selenomethionine derivative **11**, on the other hand, provided clean and complete triazole formation with no loss of particle integrity (Table 2, entry 10), showing again that triazole moieties are well tolerated by the Qβ capsid.

CONCLUSIONS

We describe here the first successful site-specific incorporation and subsequent reaction of unnatural amino acids into virus-like particles. The substitutions of azide- and alkyne-containing structures for methionine had no apparent effect on the ability of the resulting proteins to self-assemble into icosahedral capsids that are indistinguishable in structure from the native forms. Tight control over protein expression in methionine auxotrophic cells resulted in high yields of the assembled capsids. The degree of post-translational removal of unnatural amino acid introduced in position 1 in place of Met was variable, and was characterized by trypsin digestion and mass spectrometry analysis.

These novel capsids can be chemically addressed with perfect chemoselectivity by the CuAAC reaction. HBV was found to be sensitive to the coupling of molecules to the 4-helix-bundle spikes, while Qβ suffered from much fewer limitations in this regard. The low concentrations of azide and alkyne reagents required for coverage of most or all of the inserted azide and alkyne groups are made possible by the efficiency of the CuAAC process. Because the CuAAC reaction is insensitive to the substituents present on the azide and alkyne reactants and similarly unreactive with natural protein functional groups, the two-step process of genetically directed incorporation of azides or alkynes followed by CuAAC ligation provides a functional equivalent to the installation of almost any unnatural (triazole-linked) amino acid one can imagine.

EXPERIMENTAL PROCEDURES

CP149 HBV Plasmid Construction

A pET11c plasmid containing the Cp149 sequence was gratefully received from Prof. Adam Zlotnick of the Oklahoma University Health Sciences Center. In order to provide tight inducible control overexpression (pET11c was found to be constitutively expressed to an unacceptable degree), the HBV gene was amplified using the following primers: Cp149F 5′-AAG AAG GAG GAT ATA **GGT CTC AC** ATG GAC ATT GAC CCT-3′ and Cp149R 5′-TCG GGC TTT GTT AGC AGC CGG **AAG CTT** ATA CTA AAC AAC CGT-3′ The PCR product was sequentially digested with Hind III and Bsa I, and then ligated into pQE-60 plasmid (Qiagen) which had been sequentially digested with Hind III and Nco I. The resulting plasmid was transformed into competent M15MA cells harboring the pREP4 plasmid yielding the expression cells M15MA(pQE-60/HBV).

Site-Directed Mutagenesis of Cp149 HBV

Mutations were introduced into the coat protein of HBV by standard overlap PCR to remove the methionine at position 66 (M66S). The following general forward and reverse primers were

used: Forward 5′-AGA ATT CAT TAA AGA GGA GAA ATT AAC-3′, Reverse 5′-CCA AGC TCA GCT AAT GCT TAT CCT-3′, M66SF 5′-GGA GAC TTA TCT ACT CTA GCT-3′, M66SR 5′-AGC TAG AGT AGA TAA GTC TCC-3′. The PCR products were sequentially digested with Hind III and NcoI and ligated into pQE-60 that had previously been digested with Hind III and Nco I. The resulting plasmids were transformed into competent M15MA cells yielding the following expression construct: M15MA(pQE-60/M66S HBV).

Insertion of the K16 M Q*β* Coat Protein Gene into pQE-60

The coat protein gene for Q*β* containing the point mutation K16 M was originally created in the pET-28b plasmid, which is not compatible with expression in M15 based Met auxotrophic *E. coli* cells. Therefore, the Q*β* coat protein gene was amplified from the pET-28b plasmid using the following primers: QBF 5′-AAA GAG GAG AAA TTA AGG TCT CAC ATG GCA AAA TTA GAG ACT-3′ and QBR 5′-CCA AGC TCA GCT AAT T**AA GCT T**TA TTA ATA-3′ The PCR product was sequentially digested with Hind III and Bsa I. The digested PCR product was ligated into pQE-60 plasmid (Qiagen), which had been sequentially digested with Hind III and Nco I. The resulting plasmid was transformed into competent M15MA cells harboring the pREP4 plasmid yielding the expression cells M15MA(pQE-60/Q*β* K16M).

Site-Directed Mutagenesis of K16 M Q*β*

The following primers were used to introduce Met at position 93 (T93M), using standard overlap PCR as above: Forward 5′-AGA ATT CAT TAA AGA GGA GAA ATT AAC-3′, Reverse 5′-CCA AGC TCA GCT AAT GCT TAT CCT-3′, WTF 5′-GGA GAC TTA TCT ACT CTA GCT-3′, WTR 5′-AGC TAG AGT AGA TAA GTC TCC-3′. The PCR products were sequentially digested with Hind III and NcoI and ligated into pQE-60 that had previously been digested with Hind III and Nco I. The resulting plasmids were transformed into competent M15MA cells yielding the following expression construct: M15MA(pQE-60/WT Q*β*) and M15MA(pQE-60/T93 M Q*β*).

Synthesis of Unnatural Amino Acids (1 and 2)

Several short routes to azidohomoalanine (**1**) have been reported in the literature (15,65-67). We chose a simplified version of the method of Rappoport and co-workers (68), since the starting lactone is commercially available in racemic form at modest cost and an enantiospecific synthesis is not required because *E. coli* incorporates only the L-isomer during protein expression. α-Amino-γ-butyrolactone hydrobromide (5.02 g, 27.6 mmol) was refluxed in 1:1 HBr/glacial HOAc (250 mL) overnight (17−24 h). The HBr and acetic acid were then removed by rotary evaporation, yielding crude bromohomoalanine. The crude material was then dissolved in a solution of NaN_3 (9.00 g, 138 mmol) in water (125 mL) and refluxed again overnight. The solution was evaporated to dryness and the residual tan solid resuspended in a minimal volume of 0.1 M HCl. The acidic solution was passed through a column of Dowex 50WX4−100 ion-exchange resin, washing with water and eluting the product with 1 M NH_4OH. The collected fractions were evaporated to dryness, yielding an oil. Compound **1** was obtained as a tan solid (1.49 g, 10.3 mmol, 37%) upon resuspending in a minimal volume of water and lyophilizing. The purity of the solid was determined by NMR using pyridine as an internal standard and generally was >85% (overall yields 32−38%). ^{1}H NMR (D_2O, 200 MHz, d_1 = 10 s) δ 3.44 (t, 2H, $CHC\underline{H}_2CH_2N_3$), 3.07 (dd, 1H, $C\underline{H}CH_2CH_2N_3$), 1.58 (m, 2H, $CHC\underline{H}_2CH_2N_3$). Homopropargylglycine (**2**) was prepared as previously described (10).

Incorporation of 1 into HBV and Q*β*

A single of colony of cells expressing the desired HBV or Q*β* construct was used to inoculate 5 mL of SOB media containing carbenicillin (100 μg/mL) and kanamycin (50 μg/mL) and was grown overnight. The resulting culture was transferred into 500 mL of M9 minimal media

supplemented with all 20 amino acids, carbenicillin (100 μg/mL), and kanamycin (100 μg/mL) and allowed to grow for 8 h. Aliquots (25 mL) of the resulting culture were transferred into each of 11 flasks containing 500 mL of fresh minimal media supplemented with all 20 amino acids, carbenicillin (100 μg/mL) and kanamycin (100 μg/mL) and allowed to grow overnight. In the morning the cells were pelleted and resuspended in 500 mL of fresh M9 minimal media supplemented with all of the natural amino acids minus methionine. The cells were agitated at 37 °C for 30−40 min, and then transferred into new flasks of M9 minimal media supplemented with all of the natural amino acids minus methionine, IPTG (1 mM), carbenicillin (100 μg/mL), kanamycin (100 μg/mL), and azidohomoalanine (80 mg of racemate). After 6 h at 37 °C, the cells were harvested and stored at −80 °C.

For each preparation, 30−60 g of cells were allowed to thaw at room temperature and were resuspended in 50 mL distilled water. Cold lysis buffer (200 mL, 50 mM HEPES pH 8.0, 500 mM NaCl, 0.1 mg/mL DNase1, and 0.1 mg/mL RNaseA) was added and the cells were subjected to three cycles of sonication (2 min sonication and 2 min rest per cycle). Lysozyme (1 mg per mL of lysis buffer) was added and the solution was stirred in the cold room for 1 h. Insoluble cell debris was removed by centrifugation at 10 000 rpm for 30 min in a JA-10 rotor (Beckman).

For HBV, ammonium sulfate was added to the supernatant to a final concentration of 40% of saturation, and allowed to stir at room temperature for 30 min. The precipitated HBV coat protein was separated by centrifugation (10 000 rpm, 30 min, JA-10 rotor), and then was resuspended in 0.1 M potassium phosphate buffer (50 mL, pH 7.0). Any remaining insoluble material was removed by centrifugation (10 000 rpm, 15 min, JA-17 rotor). Sodium chloride was added to a final concentration of 0.5 M and the HBV coat proteins were allowed to assemble overnight. The resulting assembled VLPs were separated from smaller proteins by ultrapelleting (42 000 rpm, 6 h, 4 °C, 50.2Ti rotor, L90K ultracentrifuge). The pelleted material was resus-pended in 3−10 mL of 0.1 M potassium phosphate buffer (pH 7.0). Further purification was accomplished by the use of two successive sucrose gradient sedimentations (10−40% sucrose gradients in SW28 rotor at 28 000 rpm for 6 h at 4 °C.

For Qβ, PEG 8000 was added to the supernatant to a final concentration of 10% and the mixture was allowed to stir at room temperature for 30 min. The precipitated Qβ capsids were separated by centrifugation (10 000 rpm, 30 min, JA-10 rotor), and then resuspended in 0.1 M potassium phosphate buffer (50 mL, pH 7.0). Insoluble material was removed by centrifugation (10 000 rpm, 15 min, JA-17 rotor), and VLPs were isolated and purified as for HBV above, with final concentration by ultrapelleting.

Characterization of HBV and Qβ Particles

All protein preparations were analyzed by denaturing gel electrophoresis (4−12% NuPAGE Bis-Tris gel, Invitrogen) to estimate their purity; in all cases, the anticipated coat protein band constituted >95% of the intensity visualized by densitometry after Coomassie blue staining. HBV concentration was determined by absorbance at 280 nm, 1 mg/mL providing an absorbance value of 1.74. The concentrations of modified HBV and all Qβ particles were determined with the Modified Bradford Assay (Pierce, Inc.) and a BSA standard curve. Since HBV VLPs do not contain significant quantities of RNA, the ratio of absorbances at 260 nm vs 280 nm was 0.6−0.7. Qβ VLPs package random cellular nucleic acid, giving rise to A_{260}/A_{280} values of 1.8−1.9. The presence of individual, aggregated, and disassembled particles was determined by size-exclusion chromatography on a Superose 6 column using an Akta Explorer (GE Healthcare) fast protein liquid chromatography (FPLC) instrument. Transmission electron microscopy was performed by applying particles at a concentration of 0.2 mg/mL to a carbon-coated Formvar transmission electron grid. The grids were stained with 2% uranyl acetate, and visualized in a Phillips CM120 transmission electron microscope.

VLP samples were processed for determination of derivatization site(s) by MALDI mass spectrometry as follows. Samples (100 μL, 1−2 mg/mL protein) were mixed with 300 μL of 8 M urea and 30 μL of 1 M DTT, and incubated at 37 °C for 1 h to allow the protein to denature. Iodoacetamide (1 M, 50 μL) was added to cap any free cysteines and the sample was again incubated at 37 °C for 1 h. DTT (30 μL) was added to quench unreacted capping reagent, and the samples were diluted to a final volume of 1.9 mL using 25 mM ammonium bicarbonate (pH 8.0). Each sample was digested with 30 μg of either trypsin or Glu-C protease overnight at 37 °C. The samples were then concentrated to approximately 300 μL, and urea was removed with Zip-tips (Microcon) prior to MALDI analysis.

Cryoelectron Microscopy and Analysis

Samples were prepared for CryoEM analysis by preservation in vitreous ice via rapid-freeze plunging onto plasma cleaned Cflat carbon film grids using a Vitrobot (FEI Co). Data collection was performed on Tecnai F20 electron microscopes (FEI Co.) operating at 120 keV using a dose of ~20e^{-}/Å^2 and a nominal underfocus of 0.8 to 3 μm utilizing the Leginon data collection software (69). For the reconstructions, 735 micrographs of azidohomoalanine-incorporated HBV were collected at a nominal magnification of 80 000× at a pixel size of 0.14 nm at the specimen. 125 micrographs of azidohomoalanine-incorporated Qβ particles were collected at a nominal magnification of 50 000× at a pixel size of 0.23 nm at the specimen. All micrographs were collected on a 4000 × 4000 CCD camera (Gatan Inc.). CryoEM analysis of all other Qβ variants, including the transferrin-alkyne conjugated particles, was performed under the same conditions as the azidohomoalanine-incorporated HBV particles.

The contrast transfer function (CTF) for each micrograph was estimated using the Automated CTF Estimation (ACE) package (70). 8906 HBV particles and 11 882 Qβ particles were extracted from the collected data at a box size of 304 × 304 pixels and 180 × 180 pixels, respectively. The HBV particles were binned by a factor of 2 for the reconstruction. Phase correction of the single particles and subsequent three-dimensional refinement was carried out with the EMAN software package (71). The amplitudes of the resulting refined structures were adjusted with the SPIDER software package (72). Resolution of the final HBV and Qβ densities were determined to be around 8 Å and 10 Å (respectively) according to 0.5 FSC criteria. Rigid-body docking of crystal structures into the reconstruction density and graphical representations were produced by the Chimera visualization software package (73,74).

Copper Catalyzed Azide-Alkyne Cycloaddition Reactions

Purified azide-containing HBV or Qβ particles were pelleted out of solution (42 000 rpm, 6 h), the supernatant was removed, and residual buffer was allowed to drain away from the pellet. The viral pellet was then taken into a nitrogen-filled glovebox (without exposure to vacuum) and resuspended in a minimal volume of degassed 0.1 M Tris at pH 8.0. A small aliquot of the virus solution was removed from the glovebox and used to determine virus concentration. A typical conjugation reaction employed a VLP concentration of 2 mg/mL in 0.1 M Tris (pH 8.0) in a round-bottomed 2 mL Eppendorf tube (rather than conical tubes that do not provide good mixing upon gentle agitation). Fluorescein alkyne **6** (final concentration 1 mM) was added, followed by a freshly prepared buffer solution of Cu(I) triflate and 2 equiv of ligand **4** or **5**. Final concentrations of Cu were either 100 μM or 250 μM for HBV, 500 μM or 1 mM for Qβ. The tube was sealed, placed in a secondary sealed container (usually a small round-bottomed flask), removed from the glovebox, and attached to a slow tumbler arm for agitation at room temperature for 16−18 h. After completion of the reaction, intact virus-like particles were separated from excess labeling reagent using a combination of 10−40% sucrose gradients (38 000 rpm, SW41 rotor, 4 h for HBV, 3 h for Qβ) and ultrapelleting.

ACKNOWLEDGMENT

This work was supported by the NIH (AI056013, RR021886, GM62523), the David & Lucille Packard Foundation Interdisciplinary Science Program, and the Canadian Institutes of Health Research (postdoctoral fellowship to A.K.U.).Cryo-electron microscopy was performed at the National Resource for Automated Molecular Microscopy which is supported by the NIH NCRR P41 program (RR17573).

LITERATURE CITED

1. Noren CJ, Anthony-Cahill SJ, Griffith MC, Schultz PG. A general method for site-specific incorporation of unnatural amino acids into proteins. Science 1989;244:182–188. [PubMed: 2649980]
2. Cornish VW, Benson DR, Altenbach CA, Hideg K, Hubbell WL, Schultz PG. Site-specific incorporation of biophysical probes into proteins. Proc. Natl. Acad. Sci. USA 1994;91:2910–2914. [PubMed: 8159678]
3. Wang L, Brock A, Herberich B, Schultz PG. Expanding the genetic code of *Escherichia coli.* Science 2001;292:498–500. [PubMed: 11313494]
4. Anderson JC, Schultz PG. Adaptation of an orthogonal archaeal leucyl-tRNA and synthetase pair for fourbase, amber, and opal suppression. Biochemistry 2003;42:9598–9608. [PubMed: 12911301]
5. Chin JW, Cropp TA, Anderson JC, Mukherji M, Zhang Z, Schultz PG. An expanded eukaryotic genetic code. Science 2003;301:964–967. [PubMed: 12920298]
6. Deiters A, Cropp TA, Mukherji M, Anderson JC, Schultz Peter G. Adding amino acids with novel reactivity to the genetic code of *Saccharomyces cerevisiae*. J. Am. Chem. Soc 2003;125:11782–11783. [PubMed: 14505376]
7. Tian F, Tsao M-L, Schultz PG. A phage display system with unnatural amino acids. J. Am. Chem. Soc 2004;125:15962–15963. [PubMed: 15584720]
8. Ryu Y, Schultz PG. Efficient incorporation of unnatural amino acids into proteins in *Escherichia coli*. Nat. Methods 2006;3:263–265. [PubMed: 16554830]
9. Anderson JC, Wu N, Santoro SW, Lakshman V, King DS, Schultz PG. An expanded genetic code with a functional quadruplet codon. Proc. Natl. Acad. Sci. USA 2004;101:7566–7571. [PubMed: 15138302]
10. Van Hest JCM, Kiick KL, Tirrell DA. Efficient incorporation of unsaturated methionine analogues into proteins in vivo. J. Am. Chem. Soc 2000;122:1282–1288.
11. Kiick KL, Tirrell David A. Protein engineering by *in vivo*incorporation of non-natural amino acids: Control of incorporation of methioonine analogues by methionyl tRNA synthetase. Tetrahedron 2000;56:9487–9493.
12. Kiick K,L, Weberskirch R, Tirrell DA. Identification of an expanded set of translationally active methionine analogues in *Escherichia coli*. FEBS Lett 2001;502:25–30. [PubMed: 11478942]
13. Kiick KL, Saxon E, Tirrell DA, Bertozzi CR. Incorporation of azides into recombinant proteins for chemoselective modification by the Staudinger ligation. Proc. Natl. Acad. Sci. USA 2002;99:19–24. [PubMed: 11752401]
14. Link AJ, Tirrell DA. Cell surface labeling of *Escherichia coli* via copper(I)-catalyzed [3 + 2] cycloaddition. J. Am. Chem. Soc 2003;125:11164–11165. [PubMed: 16220915]
15. Link AJ, Vink MKS, Tirrell DA. Presentation and detection of azide functionality in bacterial cell surface proteins. J. Am. Chem. Soc 2004;126:10598–10602. [PubMed: 15327317]
16. Link AJ, Tirrell DA. Reassignment of sense codons *in vivo*. Methods 2005;36:291–298. [PubMed: 16076455]
17. Link AJ, Vink MKS, Agard NJ, Prescher JA, Bertozzi CR, Tirrell DA. Discovery of aminoacyl-tRNA synthetase activity through cell-surface display of non-canonical amino acids. Proc. Natl. Acad. Sci. USA 2006;103:10180–10185. [PubMed: 16801548]
18. van Hest JCM, Tirrell DA. Efficient introduction of alkene functionality into proteins *in vivo*. FEBS Lett 1998;428:68–70. [PubMed: 9645477]
19. Kiick KL, Van Hest JCM, Tirrell DA. Expanding the scope of protein biosynthesis by altering the methionyl-tRNA synthetase activity of a bacterial expression host. Angew. Chem., Int. Ed 2000;39:2148–2152.

20. Tang Y, Tirrell DA. Biosynthesis of a highly stable coiled-coil protein containing hexafluoroleucine in an engineered bacterial host. J. Am. Chem. Soc 2001;123:11089–11090. [PubMed: 11686725]
21. Wang Q, Chan TR, Hilgraf R, Fokin VV, Sharpless KB, Finn MG. Bioconjugation by copper(I)-catalyzed azide-alkyne [3 + 2] cycloaddition. J. Am. Chem. Soc 2003;125:3192–3193. [PubMed: 12630856]
22. Yoshikawa E, Fournier MJ, Mason TL, Tirrell DA. Genetically Engineered fluoropolymers. Synthesis of repetitive polypeptides containing p-fluorophenylalanine residues. Macromolecules 1994;27:5471–5475.
23. Budisa N, Alefelder S, Bae JH, Golbik R, Minks C, Huber R, Moroder L. Proteins with β-(thienopyrrolyl)alanines as alternative chromophores and pharmaceutically active amino acids. Protein Sci 2001;10:1281–1292. [PubMed: 11420430]
24. Bae JH, Alefelder S, Kaiser JT, Friedrich R, Moroder L, Budisa N. Incorporation of β-seleno(3,2-b) pyrrolyl-alanine into proteins for phase determination in protein X-ray crystallography. J. Mol. Biol 2001;309:925–936. [PubMed: 11399069]
25. Renner C, Alefelder S, Bae JH, Budisa N, Huber R, Moroder L. Fluoroprolines as tools for protein design and engineering. Angew. Chem., Int. Ed 2001;40:923–925.
26. Link AJ, Mock ML, Tirrell DA. Noncanonical amino acids in protein engineering. Curr. Opin. Biotechnol 2003;14:603–609. [PubMed: 14662389]
27. Saxon E, Bertozzi Carolyn R. Cell surface engineering by a modified Staudinger reaction. Science 2000;287:2007–2010. [PubMed: 10720325]
28. Vocadlo DJ, Bertozzi CR. A strategy for functional proteomic analysis of glycosidase activity from cell lysates. Angew. Chem., Int. Ed 2004;43:5338–5342.
29. Agard NJ, Baskin JM, Prescher JA, Lo A, Bertozzi CR. A comparative study of bioorthogonal reactions with azides. ACS Chem. Biol 2006;1:644–648. [PubMed: 17175580]
30. Mahal LK, Yarema KJ, Bertozzi Carolyn R. Engineering chemical reactivity on cell surfaces through oligosaccharide biosynthesis. Science 1997;276:1125–1128. [PubMed: 9173543]
31. Agard NJ, Prescher Jennifer A, Bertozzi Carolyn R. A strain-promoted (3 + 2) azide-alkyne cycloaddition for covalent modification of biomolecules in living systems. J. Am. Chem. Soc 2004;126:15046–15047. [PubMed: 15547999]
32. Rostovtsev VV, Green LG, Fokin VV, Sharpless KB. A stepwise Huisgen cycloaddition process: Copper(I) catalyzed regioselective “ligation” of azides and terminal alkynes. Angew. Chem., Int. Ed 2002;41:2596–2599.
33. Tornøe CW, Christensen C, Meldal M. Peptidotriazoles on solid phase: [1,2,3]-triazoles by regiospecific copper(I)-catalyzed 1,3-dipolar cycloadditions of terminal alkynes to azides. J. Org. Chem 2002;67:3057–3062. [PubMed: 11975567]
34. Wang Q, Chan TR, Hilgraf R, Folkin VV, Sharpless KB, Finn MG. Bioconjugation by copper(I)-catalyzed azide-alkyne (3 + 2) cycloaddition. J. Am. Chem. Soc 2003;125:3192–3193. [PubMed: 12630856]
35. Sen Gupta S, Kuzelka J, Singh P, Lewis WG, Manchester M, Finn MG. Accelerated bioorthogonal conjugation: a practical method for the ligation of diverse functional molecules to a polyvalent virus scaffold. Bioconjugate Chem 2005;16:1572–1579.
36. Deiters A, Cropp TA, Summerer D, Mukherji M, Schultz PG. Site-specific PEGylation of proteins containing unnatural amino acids. Bioorg. Med. Chem. Lett 2004;14:5743–5745. [PubMed: 15501033]
37. Kaltgrad E, Sen Gupta S, Punna S, Huang C-Y, Chang A, Wong C-H, Finn MG, Blixt O. Anticarbohydrate antibodies elicited by polyvalent display on a viral scaffold. ChemBioChem 2007;8:1455–1462. [PubMed: 17676704]
38. Prasuhn JDE, Yeh RM, Obenaus A, Manchester M, Finn MG. Viral MRI contrast agents: coordination of Gd by native virions and attachment of Gd complexes by azide-alkyne cycloaddition. Chem. Commun 2007;12:1269–1271.
39. Singh P, Prasuhn DEJ, Yeh RM, Destito G, Rae CS, Osborn K, Finn MG, Manchester M. Biodistribution, toxicity and pathology of cowpea mosaic virus nanoparticle in vivo. J. Controlled Release 2007;120:41–50.

40. Beatty KE, Xie F, Wang Q, Tirrell DA. Selective dye-labeling of newly synthesized proteins in bacterial cells. J. Am. Chem. Soc 2005;127:14150–14151. [PubMed: 16218586]
41. Dieterich DC, Link AJ, Graumann J, Tirrell DA, Schuman EM. Selective identification of newly synthesized proteins in mammalian cells using bioorthogonal noncanonical amino acid tagging (BONCAT). Proc. Natl. Acad. Sci. USA 2006;103:9482–9487. [PubMed: 16769897]
42. Beatty KE, Liu JC, Xie F, Dieterich DC, Schuman EM, Wang Q, Tirrell David A. Fluorescence visualization of newly synthesized proteins in mammalian cells. Angew. Chem., Int. Ed 2006;45:7364–7367.
43. Dieterich DC, Lee JJ, Link AJ, Graumann J, Tirrell David A, Schuman EM. Labeling, detection, and identification of newly synthesized proteomes with bioorthogonal non-canonical amino acid tagging. Nat. Prot 2007;2:532–540.
44. Speers AE, Cravatt BF. Profiling enzyme activities *in vivo* using click chemistry method. Chem. Biol 2004;11:535–546. [PubMed: 15123248]
45. Speers AE, Adam GC, Cravatt BF. Activity based protein profiling *in vivo* using a copper(I)-catalyzed azide-alkyne cycloaddition. J. Am. Chem. Soc 2003:125.
46. Kenney JM, von Bonsdorff C-H, Nassal M, Fuller SD. Evolutionary conservation in the hepatitis B virus core structure: comparison of human and duck cores. Structure 1995;3:1009–1019. [PubMed: 8589996]
47. Wynne SA, Crowther RA, Leslie AG. The crystal structure of human hepatitis B virus. Mol. Cell 1999;6:771–780. [PubMed: 10394365]
48. Hilditch CM, Rogers LJ, Bishop DHL. Physicochemical analysis of the hepatitis B virus core antigen produced by a baculovirus expression vector. J. Gen. Virol 1990;71:2755–2759. [PubMed: 2254755]
49. Allen M, Bulte JWM, Liepold L, Basu G, Zywicke HA, Frank JA, Young M, Douglas T. Paramagnetic viral nanoparticles as potential high-relaxivity magnetic resonance contrast agents. Magn. Res. Med 2005;54:807–812.
50. Cohen BJ, Richmond JE. Electron microscopy of hepatitis B core antigen synthesized in *E. coli*. Nature 1982;296:677–678. [PubMed: 7040981]
51. Wingfield PT, Stahl SJ, Williams RW, Steven AC. Hepatitis core antigen produced in *Escherichia coli*: subunit composition, conformational analysis, andin vitro capsid assembly. Biochemistry 1995;34:4919–4932. [PubMed: 7711014]
52. Vallegaard K, Fridborg K, Liljas L. Crystallization and preliminary x-ray diffraction studies of the bacteriophage Q*β*. Acta Crystallogr., Sect. D: Biol. Cryst 1994;D50:105–109.
53. Tars K, Bundule M, Fridborg K, Liljas L. The crystal structure of bacteriophage GA and a comparison of bacteriophages belonging to the major groups of *Escherichia coli* leviviruses. J. Mol. Biol 1997;271:759–773. [PubMed: 9299325]
54. Overby LR, Barlow GH, Doi RH, Jacob M, Spiegelman S. Comparison of two serologically distinct ribonucleic acid bacteriophages. J. Bacteriol 1966;91:442–448. [PubMed: 5903109]
55. Golmohammadi R, Fridborg K, Bundule M, Valegaard K, Liljas L. The crystal structure of bacteriophage Q*β* at 3.5 Å resolution. Structure 1996;4:543–554. [PubMed: 8736553]
56. Kozlovska TM, Cielens I, Dreilinna D, Dislers A, Baumanis V, Ose V, Pumpens P. Recombinant RNA phage Q*β* capsid particles synthesized and self-assembled in *Escherichia coli*. Gene 1993;137:133–137. [PubMed: 7506687]
57. Vasiljeva I, Kozlovska T, Cielens I, Strelnikova A, Kazaks A, Ose V, Pumpens P. Mosaic Q*β* coats as a new presentation model. FEBS Lett 1998;431:7–11. [PubMed: 9684855]
58. Freivalds J, Dislers A, Ose V, Skrastina D, Cielens I, Pumpens P, Sasnauskas K, Kazaks A. Assembly of bacteriophage Q*β* virus-like particles in yeast *Saccharomyces cerevisiae* and *Pichia pastoris*. J. Biotechnol 2006;123:297–303. [PubMed: 16406160]
59. Shepherd CM, Borelli IA, Lander G, Natarajan P, Siddavanahalli V, Bajaj C, Johnson JE, Brooks CL III, Reddy VS. VIPERdb: a relational database for structural virology. Nucleic Acids Res 2006;34:D386–D389. [PubMed: 16381893]
60. Hirel P-H, Schmitter J-M, Dessen P, Fayat G, Blanquet S. Extent of *N*-terminal methionine excision from *Escherichia coli* proteins is governed by the side-chain length of the penultimate amino acid. Proc. Natl. Acad. Sci. USA 1989;86:8247–8251. [PubMed: 2682640]

61. Lewis WG, Magallon FG, Fokin VV, Finn MG. Discovery and characterization of catalysts for azide-alkyne cycloaddition by fluorescence quenching. J. Am. Chem. Soc 2004;126:9152–9153. [PubMed: 15281783]
62. Sen Gupta S, Raja KS, Kaltgrad E, Strable E, Finn MG. Virus-glycoploymer conjugates by copper (I)-catalysis of atom transfer radical polymerization and azide-alkyne cycloaddition. Chem. Commun 2005:4315–4317.
63. Stray SJ, Bourne CR, Punna S, Lewis WG, Finn MG, Zlotnick A. A heteroaryldihydropyrimidine activates and can misdirect hepatitis B virus capsid assembly. Proc. Natl. Acad. Sci. USA 2005;102:8138–8143. [PubMed: 15928089]
64. Bourne CR, Finn MG, Zlotnick A. Global structural changes in hepatitis B virus capsids induced by the assembly effector HAP1. J. Virol 2006;80:11055–11061. [PubMed: 16943288]
65. Mangold JB, Mischke MR, LaVelle JM. Azidoalanine mutagenicity in *Salmonella*: Effect of homologation and α-methyl substitution. Mut. Res 1989;308:33–42. [PubMed: 7516484]
66. Link AJ, Vink MKS, Tirrell DA. Preparation of the functionalizable methionine surrogate azidohomoalanine *via* copper-catalyzed diazo transfer. Nat. Protocols 2007;2:1879–1883.
67. Link AJ, Vink MKS, Tirrell DA. Synthesis of the functionalizable methionine surrogate azidohomoalanine using Boc-homoserine as precursor. Nat. Protocols 2007;2:1884–1887.
68. McLaughlin M, Mohareb RM, Rapoport H. An efficient procedure for the preparation of 4-substituted 5-aminoimidazoles. J. Org. Chem 2003;68:50–54. [PubMed: 12515460]
69. Suloway C, Pulokas J, Fellmann D, Cheng A, Guerra F, Quispe J, Stagg S, Potter CS, Carragher B. Automated molecular microscopy: the new Leginon system. J. Struct. Biol 2005;151:41–60. [PubMed: 15890530]
70. Mallick SP, Carragher B, Potter CS, Kriegman DJ. ACE: automated CTF estimation. Ultramicroscopy 2005;104:8–29. [PubMed: 15935913]
71. Ludtke SJ, Baldwin PR, Chiu W. EMAN: semiautomated software for high-resolution single-particle reconstructions. J. Struct. Biol 1999;128:82–97. [PubMed: 10600563]
72. Frank J, Radermacher M, Penczek P, Zhu J, Li Y, Ladjadj M, Leith A. SPIDER and WEB: processing and visualization of images in 3D electron microscopy and related fields. J. Struct. Biol 1996;116:190–199. [PubMed: 8742743]
73. Goddard TD, Huang CC, Ferrin TE. Software extensions to UCSF Chimera for interactive visualization of large molecular assemblies. Structure 2005;13:473–482. [PubMed: 15766548]
74. Goddard TD, Huang CC, Ferrin TE. Visualizing density maps with UCSF Chimera. J. Struct. Biol 2007;157:281–287. [PubMed: 16963278]

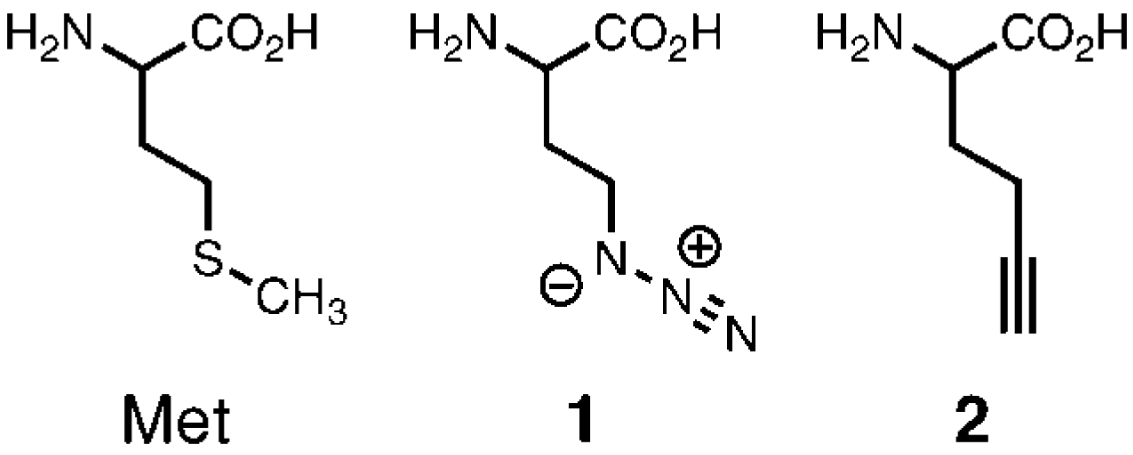

Figure 1.
Methionine analogues **1** and **2** incorporated into virus-like capsids using codon reassignment.

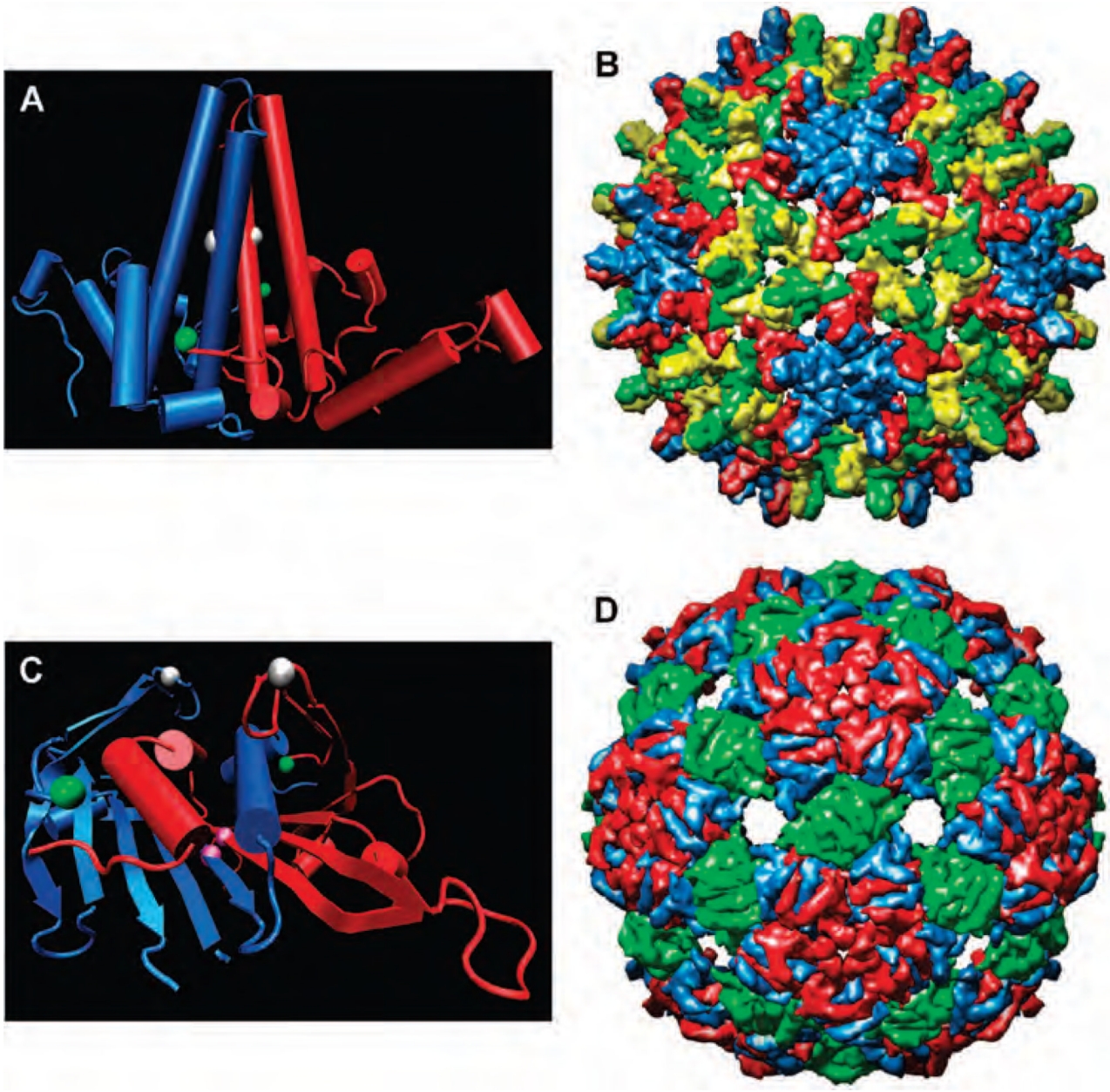

Figure 2.
HBV and Q*β* virus-like particles. (A) HBV dimer; (B) HBV virus-like particle; (C) Q*β* dimer; (D) Q*β* virus-like particle (47,55,59). Representations (A) and (C) look obliquely down onto the outside capsid surface, showing the 4-helix bundle for HBV and intertwined α-helix and loop segments over adjacent *β*-sheets for Q*β*. The spheres mark the locations of methionine residues: green = *N*-termini, white = Met66 in HBV and K16 M in Q*β*, purple = Q*β* T93M.

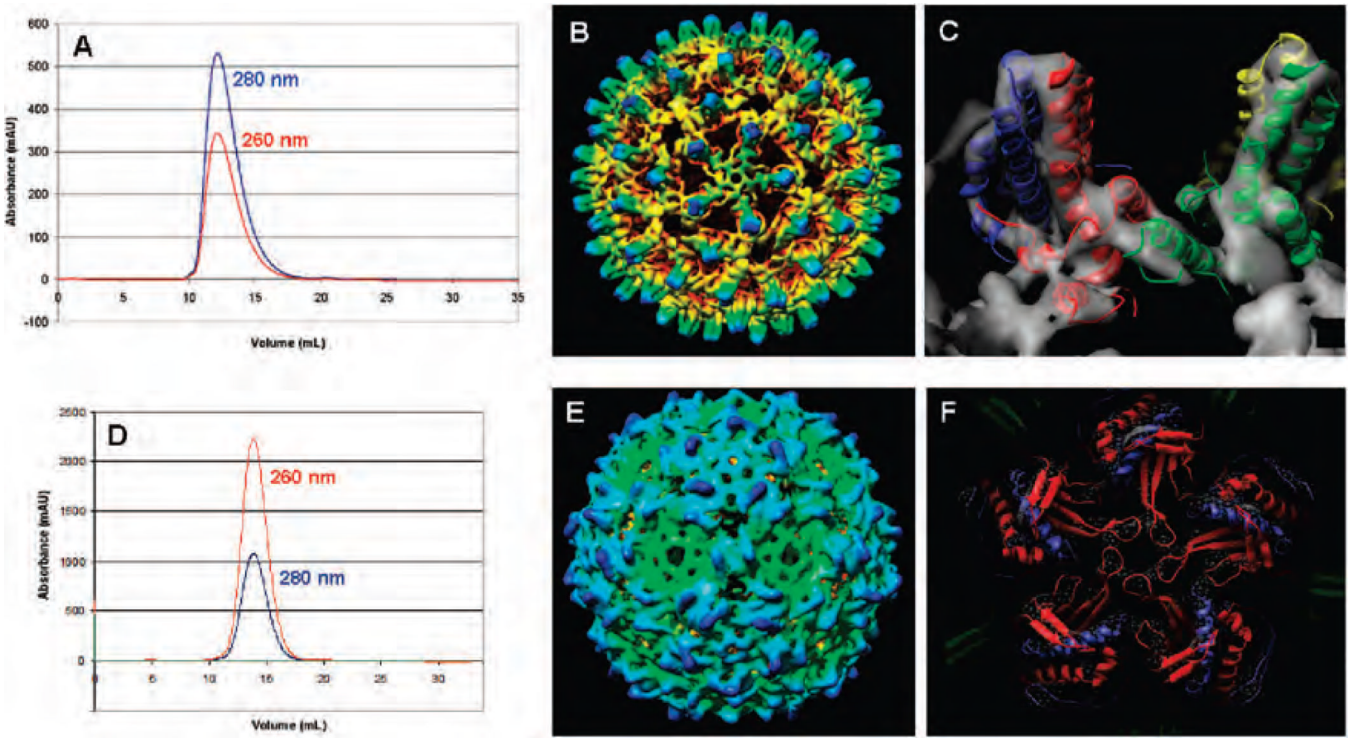

Figure 3.

Characterization of the HBV (A-C) and Qβ (D-F) capsids containing **1**. (A and D) Size exclusion chromatography (Superose-6), with retention times matching those of intact native capsids. (B and E) Cryo-electron microscopy image reconstructions. (C and F) X-ray crystal structures docked into the cryo electron density maps. Characterization data for Qβ incorporating **2** may be found in Supporting Information.

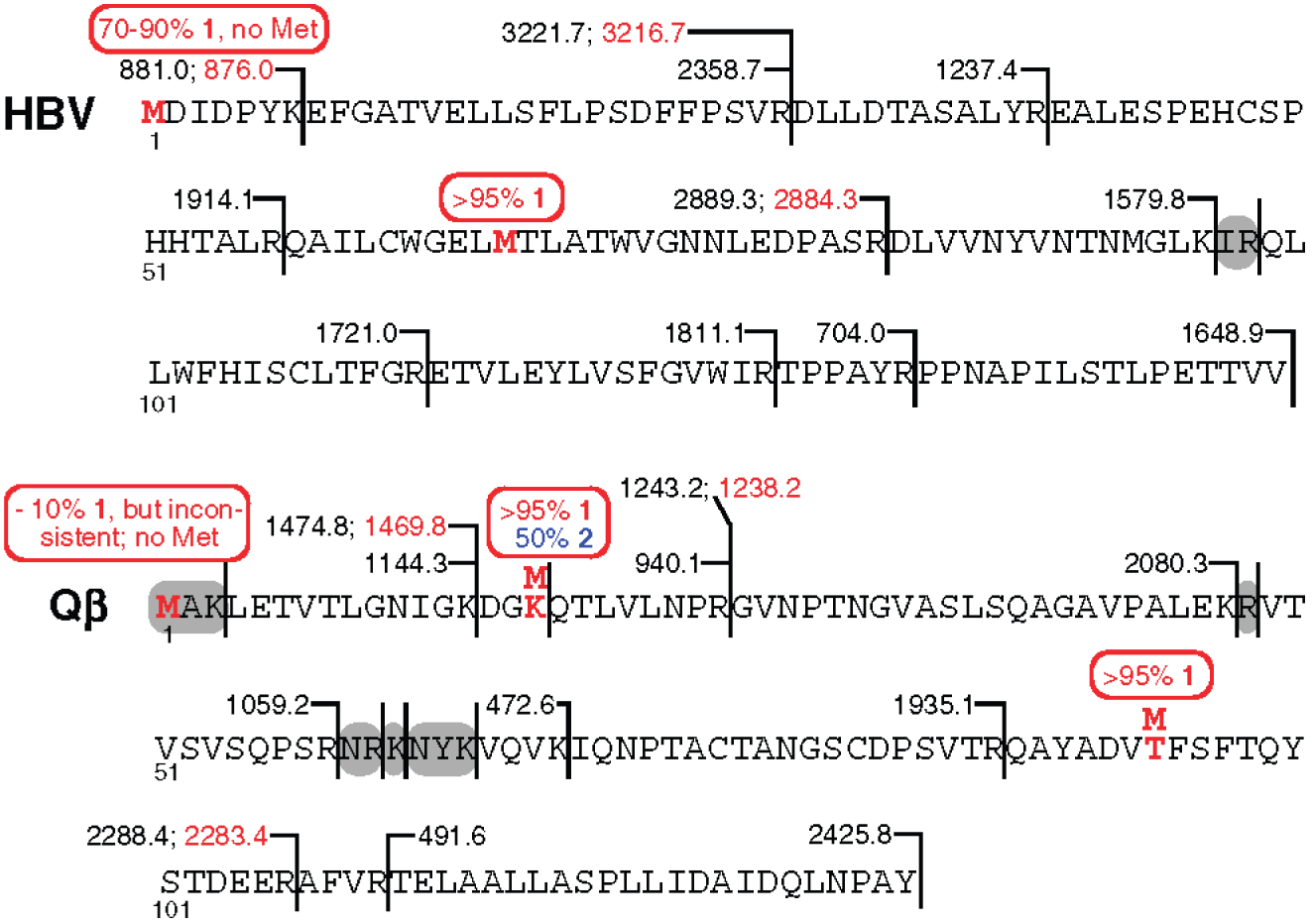

Figure 4.

Summary of results from trypsin digestion and mass spectrometry of HBV and Q*β* expressed with Met and **1** in locations marked in red. The detected fragments are indicated by the numerical values of *m*/*z* shown at the right of each; values in red are those with the unnatural amino acid incorporated. Many fused fragments (fragments derived from incomplete cleavage) were detected as well, giving rise to the same conclusions. The small peptides marked in gray were not detected. Conclusions about the level of incorporation of **1** at each indicated position are shown in the red ovals.

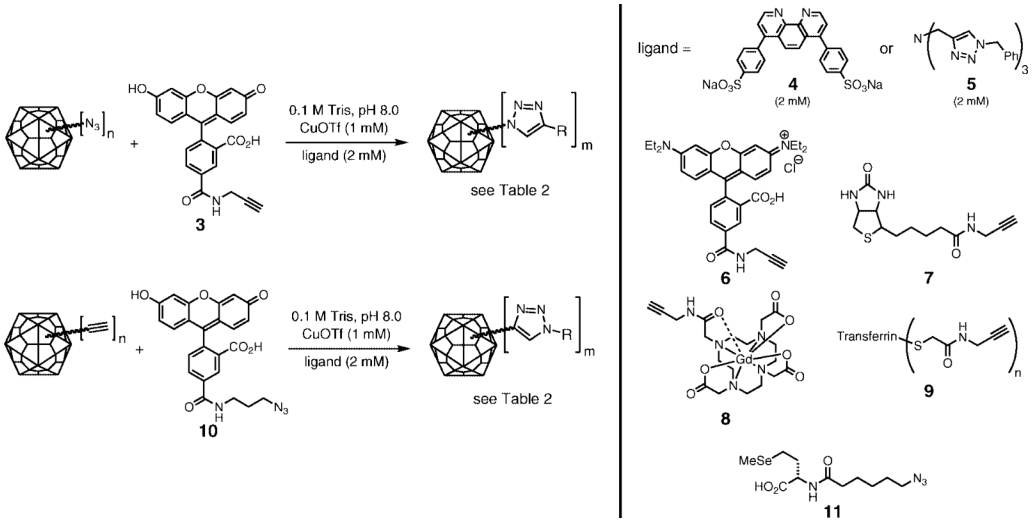

Figure 5.
Copper-catalyzed azide-alkyne cycloaddition (CuAAC) reaction of virus-like particles with alkyne or azide derivatives.

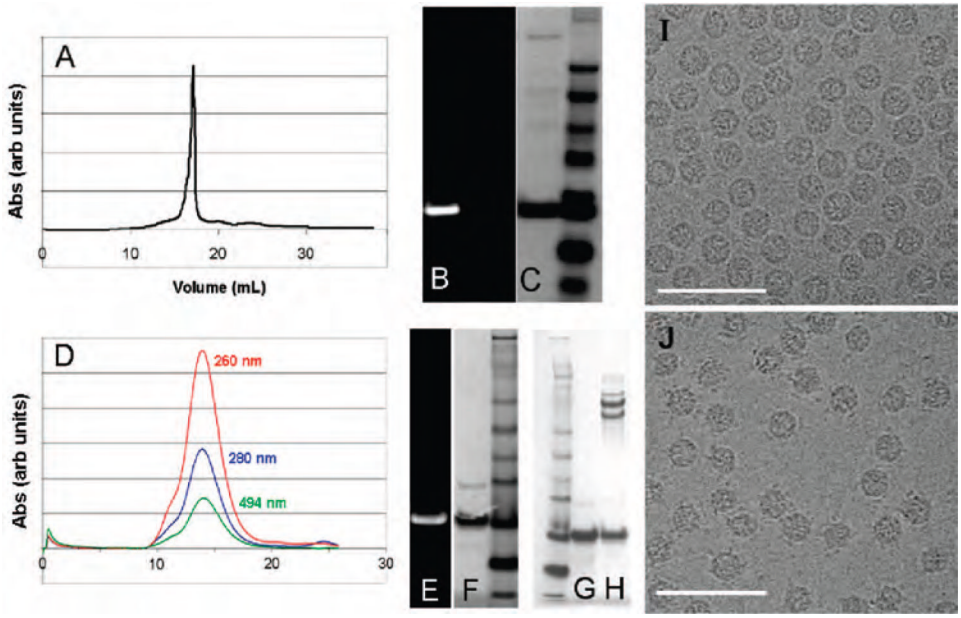

Figure 6.

Characterization of virus-like capsids after CuAAC reactions: HBV = A-C; Qβ = D-H. (A) Size exclusion chromatography showing a peak with a retention volume of 18 mL corresponding to disassembled capsid. (B,C) SDS-PAGE of the Cp149 protein isolated from the reaction, visualized under ultraviolet illumination (B) and then with Coumassie staining (C). The right lane is a molecular weight ladder. (D) Size exclusion chromatography showing an elution volume of 14 mL, characteristic of intact Qβ capsids, and coelution of fluorescein with the protein showing covalent attachment. (E,F) SDS-PAGE of the Qβ protein showing fluorescein labeling as above. (G) Same as (F). (H) SDS-PAGE of purified Qβ-transferrin conjugate; the higher molecular weight bands are in the expected position for the Cp149-transferrin fusion, with multiple bands deriving from the somewhat impure nature of the starting transferrin sample. (I) Transmission electron microscopy (TEM) image of Qβ $(1MN_3)_{9–18}(K16M\text{-}N_3)_{180}$. (J) TEM image of the same particle conjugated to transferrin-alkyne **9**, after purification. Note the appearance of spots surrounding most of the particles, due to the tethered 80 kD protein.

Table 1

Average Expression Levels of HBV and Q*β* VLPs with Methionine, Azidohomoalanine (1), or Homopropargylglycine (2)

particle[a]	amino acid	yield (mg protein per g cells)	yield (mg protein per L culture)
HBV	Met	4−5 mg/g	80−100 mg/L
HBV(1M-N_3)$_{192}$(66M-N_3)$_{240}$	**1**	1−1.5 mg/g	20−30 mg/L
HBV(M66S)	Met	4−5 mg/g	80−100 mg/L
HBV(1M-N_3)$_{102}$(M66S)	**1**	2−3 mg/g	40−60 mg/L
Q*β*	Met	3−4 mg/g	75−100 mg/L
Q*β*(1M-N_3)$_{9–18}$	**1**	2−2.4 mg/g	50−60 mg/L
Q*β*(K16M)	Met	3−4 mg/g	50−75 mg/L
Q*β*(1M-N_3)$_{9–18}$(K16M-N_3)$_{180}$	**1**	1−2 mg/g	25−35 mg/L
Q*β*(K16M-CCH)$_{90}$	**2**	2 mg/g	40 mg/L
Q*β*(T93M)	Met	3−4 mg/g	50−75 mg/L
Q*β*(1M-N_3)$_{9–18}$(T93M-N3)$_{180}$	**1**	1−2 mg/g	25−35 mg/L

[a] Nomenclature: “HBV(1M-N3)(66M-N3)” denotes HBV particles with methionines at positions 1 and 66 (which happens to be the wild-type sequence) expressed in the presence of **1** to allow azide incorporation at those residues. Other particles are designated in analogous fashion, with "CCH" replacing "N3" for those VLP's incorporating alkynyl amino acid **2**. Subscripts refer to the average number of unnatural amino acids incorporated at each position, as described in the text.

Table 2

Results of CuAAC Reactions of VLP's Containing Unnatural Amino Acids, as Shown in Figure 5

entry	particle[a]	# incorporated per particle[b]	loading[c]	recovery[d]
1	HBV(66M)	none	0	60−70%
2	HBV(1M-N_3)$_{170-215}$(66M-N_3)$_{240}$	410−455	120 ± 15[e]	≤40%
3	HBV(1M-N_3)$_{170-215}$(M66S)	170−215	120 ± 25	60−70%
4	Qβ(K16M)	none	0	75−80%
5	Qβ(1M-N_3)$_{9-18}$	9−18	15 ± 3	80−85%
6	Qβ(1M-N_3)$_{9-18}$(K16M-N_3)$_{180}$	189−198	190 ± 20	75−80%
7	Qβ(1M-N_3)$_{160}$(K16M-N_3)$_{180}$	340	306 ± 30[f]	70−80%
8	Qβ(1M-N_3)$_{9-18}$(T93M-N_3)$_{180}$	189−198	35 ± 5	75−80%
9	Qβ(K16M-CCH)$_{90}$	90	50 ± 5	20%
10	Qβ(K16M-CCH)$_{90}$	90	85 ± 5[g]	75−80%

[a] See caption to Table 1 for nomenclature.

[b] Total number of unnatural amino acids per particle, determined by trypsin digestion and mass spectrometry as described in the text.

[c] The number of attached molecules (subscripts “m” in Figure 5). Unless otherwise indicated, the value was obtained from reaction with fluorescein reagents **3** or **10** and quantitation by calibrated UV–visible absorbance of the dye (average of at least three independent reactions).

[d] Amount of purified intact capsids recovered from the reaction.

[e] More than 90% of the attachments were made at position 66.

[f] Under standard conditions; a loading of 330 ± 20 (75% recovery) was observed under the most forcing conditions tested.

[g] Reaction with azide **11**, loading determined by quantitation of attached Se atoms by inductively coupled plasma optical emission spectroscopy.